

Onset of synchronization in networks of second-order Kuramoto oscillators with delayed coupling: Exact results and application to phase-locked loops

David Métivier,^{1,*} Lucas Wetzel,^{2,†} and Shamik Gupta^{3,‡}

¹*CNLS & T-4 of Los Alamos National Laboratory, NM 87544, USA*

²*Max Planck Institute for the Physics of Complex Systems, Nöthnitzer Straße 38, D-01187 Dresden, Germany*

³*Department of Physics, Ramakrishna Mission Vivekananda Educational and Research Institute, Belur Math, Howrah 711202, India*

(Dated: April 23, 2022)

We consider the inertial Kuramoto model of N globally coupled oscillators characterized by both their phase and angular velocity, in which there is a time delay in the interaction between the oscillators. Besides the academic interest, we show that the model can be related to a network of phase-locked loops widely used in electronic circuits for generating a stable frequency at multiples of an input frequency. We study the model for a generic choice of the natural frequency distribution of the oscillators, to elucidate how a synchronized phase bifurcates from an incoherent phase as the coupling constant between the oscillators is tuned. We show that in contrast to the case with no delay, here the system in the stationary state may exhibit either a subcritical or a supercritical bifurcation between a synchronized and an incoherent phase, which is dictated by the value of the delay present in the interaction and the precise value of inertia of the oscillators. Our theoretical analysis, performed in the limit $N \rightarrow \infty$, is based on an unstable manifold expansion in the vicinity of the bifurcation, which we apply to the kinetic equation satisfied by the single-oscillator distribution function. We check our results by performing direct numerical integration of the dynamics for large N , and highlight the subtleties arising from having a finite number of oscillators.

Keywords: Spontaneous synchronization, delayed Kuramoto model, phase-locked loops

I. INTRODUCTION

A. The model

The Kuramoto model with inertia is representative of complex many-body dynamics involving a set of rotors characterized by their phases and angular velocities that are coupled all-to-all through the sine of their phase differences. Specifically, the dynamics for a system of N rotors is given by a set of $2N$ coupled first-order differential equations of the form [1–3]

$$\begin{aligned}\dot{\theta}_i(t) &= v_i(t), \\ m\dot{v}_i(t) &= -\gamma v_i(t) + \gamma\omega_i + \frac{K}{N} \sum_{j=1}^N \sin(\theta_j(t) - \theta_i(t)),\end{aligned}\tag{1}$$

where the dot denotes derivative with respect to time, $\theta_i \in [0, 2\pi)$ and v_i are the phase and the angular velocity of the i -th rotor, respectively, whose moment of inertia is $m > 0$. Here, $\gamma > 0$ is the damping constant, $K > 0$ is the coupling constant, while $\omega_i \in [-\infty, \infty]$ is the natural frequency of the i -th rotor. The frequencies $\{\omega_i\}_{1 \leq i \leq N}$ constitute a set of independent and quenched disordered random variables distributed according to a given distribution $g(\omega)$, normalized as $\int_{-\infty}^{\infty} d\omega g(\omega) = 1$ and with finite mean ω_0 . In the limit of overdamping, $\gamma/m \rightarrow \infty$, the rotors are effectively characterized by their phases alone and are therefore quite rightly referred to as oscillators [35]. In this limit, the dynamics (1) becomes that of the Kuramoto model [4–10], which over the years has emerged as a paradigmatic minimal framework to study spontaneous collective synchronization in a group of coupled limit-cycle oscillators, such as that observed in groups of fireflies flashing on and off in unison [11], in cardiac pacemaker cells [12], in Josephson junction arrays [13], in electrochemical [14] and electronic [15] oscillators, etc. The governing equations

*Electronic address: metivier@lanl.gov; These authors contributed equally to the work.

†Electronic address: lwetzel@pks.mpg.de; These authors contributed equally to the work.

‡Electronic address: shamikg1@gmail.com

of the Kuramoto model are N coupled first-order differential equations of the form

$$\gamma \dot{\theta}_i(t) = \gamma \omega_i + \frac{K}{N} \sum_{j=1}^N \sin(\theta_j(t) - \theta_i(t)). \quad (2)$$

The mean-field nature of either the dynamics (2) or the dynamics (1) becomes evident on defining the so-called synchronization order parameter $R(t)$ and the global phase $\Phi(t)$, as [4]

$$R(t)e^{i\Phi(t)} \equiv \frac{\sum_{j=1}^N e^{i\theta_j(t)}}{N}; \quad R, \Phi \in \mathbb{R}, \quad 0 \leq R \leq 1, \quad \Phi \in [0, 2\pi), \quad (3)$$

with $0 < R < 1$ characterizing a synchronized phase, and $R = 0$ an incoherent phase. In terms of $R(t)$, the dynamics (1) may be rewritten as

$$\dot{\theta}_i(t) = v_i(t), \quad (4)$$

$$m\dot{v}_i(t) = -\gamma v_i(t) + \gamma \omega_i + KR(t) \sin(\Phi(t) - \theta_i(t)),$$

which shows that the evolution of the dynamical variables at time t is governed by the value of the mean-field $R(t)e^{i\Phi(t)}$ set up collectively at time t by all the oscillators.

Both the models (1) and (2) have been extensively studied in the past and a host of results have been derived with regard to the parameter regimes allowing for the emergence of a synchronized stationary state (see Ref. [10] for a recent overview). For example, consider a $g(\omega)$ that is unimodal, namely, it is symmetric about its mean ω_0 , and decreases monotonically and continuously to zero with increasing $|\omega - \omega_0|$. In this case, it is known that in the stationary state of the dynamics (2), the system for a given choice of $g(\omega)$ may exist in either a synchronized or an incoherent phase depending on whether the coupling K is respectively above or below a critical value $K_c = 2/(\pi g(\omega_0))$; on tuning K across K_c from high to low values, one observes a *continuous* phase transition in R_{st} , the stationary value of $R(t)$. Namely, R_{st} decreases continuously from the value of unity, achieved as $K \rightarrow \infty$, to the value zero at $K = K_c$ and remains zero at smaller K values. One may interpret the transition as the case of a supercritical bifurcation, in which on tuning K , a synchronized phase bifurcates from the incoherent phase at $K = K_c$. In particular, a small change of K across K_c results in only a small change in the value of $R_{\text{st}} \propto \sqrt{K - K_c}$ close to and above K_c [4, 16]. For the same choice of a unimodal $g(\omega)$, the inertial dynamics (1) on the other hand show a *discontinuous* phase transition between synchronized and incoherent phase, where R_{st} exhibits an abrupt and big change from zero to a non-zero value on changing K by a small amount across the phase transition point [17, 18]. Here, the bifurcation of the synchronized from the incoherent phase is said to be subcritical and leads to hysteresis [19]. Thus, presence of inertia is rather drastic in that it changes completely the nature of the bifurcation and hence of the underlying stationary state.

In this work, we study for the first time the effect of a delay in the interaction between the oscillators within the framework of dynamics (1). The dynamical equations of this modified model are given by

$$\dot{\theta}_i(t) = v_i(t), \quad (5)$$

$$m\dot{v}_i(t) = -\gamma v_i(t) + \gamma \omega_i + KR(t - \tau) \sin(\Phi(t - \tau) - \theta_i(t) - \alpha),$$

thereby modeling the time-evolution which is governed by the value of the mean field at an earlier instant $t - \tau$, where $\tau > 0$ is the time delay in the interaction between the oscillators. Here, $\alpha \in (-\pi/2, \pi/2)$ is the so-called phase frustration parameter, an additional dynamical parameter that is known to affect significantly the behavior of the Kuramoto model [20]. In the overdamped limit, the model (5) reduces to

$$\gamma \dot{\theta}_i(t) = \gamma \omega_i + KR(t - \tau) \sin(\Phi(t - \tau) - \theta_i(t) - \alpha), \quad (6)$$

which in presence of additional Gaussian, white noise has been addressed in Ref. [21]. Note that for the dynamics in (6), the parameter γ may be scaled out by a redefinition of time, so that the relevant dynamical parameters are K, τ and α . In a recent work [22], two of the present authors have investigated the dynamics (6), deriving for generic $g(\omega)$ and as a function of the delay exact results for the stability boundary $K_c(\tau)$ between the incoherent and the synchronized phase and the nature in which the latter bifurcates from the former at the phase transition point (the effects of changing τ at a fixed α are the same as those from changing τ at a fixed α keeping $\alpha - \omega_0\tau$ constant). Our results imply that for a given choice of $g(\omega)$, the nature of transition (continuous versus discontinuous) between the synchronized and incoherent phases depends explicitly on the value of τ .

In view of the aforementioned developments, it is evidently of interest to investigate the effects of inertia on the time delayed model and thus embark on a detailed analysis of the dynamics (5). Since even without delay, inertia is known to have nontrivial and interesting consequences as mentioned above, we may already anticipate that an interplay of the influence of delay and inertia may result in an even richer stationary state for the dynamics (5) vis-à-vis for dynamics (6). Remarkably, the dynamics in Eq. (5), far from being just a model of academic interest, emerge naturally in the context of coupled phase-locked loops, as we now demonstrate.

B. Relation to a network of phase-locked loops

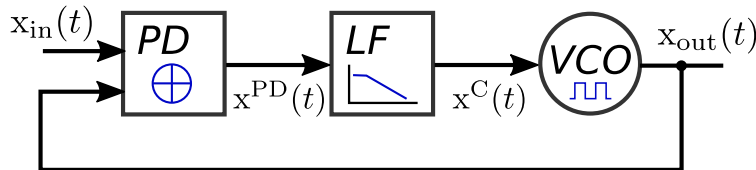


FIG. 1: Schematic diagram of a phase-locked loop (PLL). The arrows denote the direction of flow of signals in the loop.

A phase-locked loop (PLL) is an electronic component designed to generate an output signal that has a constant phase relation (and is thus locked) to the phase of its input reference. Fig. 1 shows a schematic PLL architecture consisting of a phase detector (PD), a loop filter (LF), and a voltage-controlled oscillator (VCO) acting as a variable-frequency oscillator, all connected in a feedback loop. The phase-detector output $x^{\text{PD}}(t)$ represents the phase relations of the periodic output signal $x_{\text{out}}(t)$, generated by the VCO, with the phase of the periodic input-signal $x_{\text{in}}(t)$. The loop-filtered phase-detector output yields the control signal $x^{\text{C}}(t)$ that controls the instantaneous frequency of the VCO so that its corresponding output approaches the phase and frequency of the input signal. The latter property enables a PLL to track an input frequency, or, to generate a frequency that is a multiple of the input frequency. PLL's find wide use in electronic applications as an effective device to, e.g., recover a signal from a noisy communication channel, generate a stable frequency at multiples of an input frequency, and to distribute a quartz reference clock signal via a clocktree architecture.

Let us now consider the setup of $N \geq 2$ mutually delay-coupled PLL's occupying the nodes of a network, in which the input signals for a given PLL are constituted by the delayed output received from other PLL's [23–25]. The delay could be due to transmission signaling-times, and is accounted for in the following by a discrete delay-time τ . We consider the LF to ideally damp the high-frequency components of the PD signal. Consider the output signal of the i -th PLL, $i = 1, 2, \dots, N$, in the network

$$x_i(t) = s(\theta_i(t)), \quad (7)$$

where $\theta_i(t)$ denotes the phase, and $s(\theta_i(t))$ is a 2π -periodic function with amplitude one. Depending on the type of PLL, i.e., analog or digital, the output signal may be sinusoidal or a rectangular function, respectively. The VCO is operated such that its output frequency $\dot{\theta}_i(t)$ depends linearly on the control signal $x_i^{\text{C}}(t)$:

$$\dot{\theta}_i(t) = \omega_{i,0}^{\text{VCO}} + K_i^{\text{VCO}} x_i^{\text{C}}(t), \quad (8)$$

where $\omega_{i,0}^{\text{VCO}}$ denotes the natural frequency, and K_i^{VCO} the VCO input sensitivity. The control signal is the output of the loop-filter:

$$x_i^{\text{C}}(t) = \int_0^\infty du p(u) x_i^{\text{PD}}(t-u), \quad (9)$$

where $x_i^{\text{PD}}(t)$ denotes the phase-detector signal, and $p(u)$ is the impulse response of the filter. Considering first-order loop-filters, i.e., $p(u; 1, b)$ being the Γ -distribution with shape parameter $a = 1$ and scale parameter b , the above integral equation can be rewritten by using Laplace transforms [24, 26], yielding

$$\dot{x}_i^{\text{C}}(t) = \omega_c [x_i^{\text{PD}}(t) - x_i^{\text{C}}(t)], \quad (10)$$

where ω_c denotes the cut-off frequency of the first-order low-pass filter. The initial state of the filter is given by $x_i^{\text{C}}(0) = (\dot{\theta}_i(0) - \omega_{i,0}^{\text{VCO}})/K_i^{\text{VCO}}$. The phase-detector signal depends on the type of PLL:

$$x_i^{\text{PD}}(t) = C + \frac{1}{2n(i)} \sum_{j=1}^N c_{ij} h[\theta_j(t-\tau) - \theta_i(t)], \quad (11)$$

where C is a PLL type specific offset ($C = 1/2$ for XOR PD's, while $C = 0$ for multiplier PD's), $c_{ij} = \{0, 1\}$ are the components of the adjacency matrix, with the value 1 (respectively, 0) denoting whether PLL units i and j are coupled (respectively, uncoupled), $n(i) \equiv \sum_j c_{ij}$ the total number of units coupled with unit i , $h(x)$ is a 2π -periodic coupling function, and we assumed the high-frequency components to be filtered ideally by the LF [23]. Equations (8)-(11) combined together yield a second-order phase model with delayed-coupling:

$$\frac{1}{\omega_c} \ddot{\theta}_i(t) + \dot{\theta}_i(t) = \omega_i + \frac{\tilde{K}_i}{n(i)} \sum_{j=1}^N c_{ij} h(\theta_j(t - \tau) - \theta_i(t)). \quad (12)$$

where we have defined $\omega_i \equiv \omega_{i,0}^{\text{VCO}} + C K_i^{\text{VCO}}$, and $\tilde{K}_i \equiv K_i^{\text{VCO}}/2$. The 2π -periodic coupling function h depends on the type of the PD and the corresponding input signals. Here we consider the case of a cosine coupling function, $h(x) = \cos(x)$, for analog PLL's and multiplier phase-detectors and a triangular coupling function, and $h(x) = \Delta(x)$ for digital PLL's with XOR phase-detectors. In the latter case the coupling-function can be approximated as $h(x) = -8/\pi^2 \cos(x)$. The case of a d-flip flop [36] phase detector for digital PLLs, which has a linear coupling-function, will not be considered in this work. Given these cases, we will use a sinusoidal coupling-function with a phase frustration parameter $\alpha \in [-\pi/2, \pi/2]$, that is, with $h(x) = \sin(x - \alpha)$, which represents both of the cases mentioned above. We will also specialize to the case when every PLL unit is coupled to every other, implying $c_{ij} = 1 \forall i, j = 1, 2, \dots, N$ and $n(i) = N$. Comparing Eqs. (12) and (5) leads to the correspondence $m = \omega_c^{-1}$, $\gamma = 1$, as well as $K = \tilde{K}_i$, $\alpha = \pi/2$ for the analog PLL case, and $\alpha = -\pi/2$, $K = 8\tilde{K}_i/\pi^2$ for the digital PLL approximation.

Before moving on to an analysis of the dynamics (5), it is pertinent that we give here a summary of our results obtained in this paper and the techniques employed in achieving them. We here obtain exact analytical relations for the critical point $K_c(\tau)$ beyond which the incoherent phase of the dynamics (5) becomes unstable, and furthermore, the nature in which the synchronized phase bifurcates from the incoherent phase as K is increased beyond $K_c(\tau)$. An illustration of our results for a unimodal Lorentzian distribution is shown in Fig. 2 for two representative values of the inertia, which displays both K_c and the real part of a quantity c_3 whose sign determines the nature of the bifurcation of the order parameter R , Eq. (3): a positive (respectively, a negative) sign implies a subcritical bifurcation and hence, a discontinuous transition (respective, a supercritical bifurcation and hence a continuous transition). As may be seen from the Fig. 2, K_c and the real part of c_3 both have an essential dependence on τ and m , while our analysis (see Eq. (21)) suggests that the effects of changing τ at a fixed α are the same as those from changing τ at a fixed α keeping $\alpha - \omega_0\tau$ constant.

We now summarize our method of analysis in obtaining the aforementioned results. We start off with considering the dynamics (5) in the limit $N \rightarrow \infty$, when it may be effectively characterized by a single-oscillator probability density $F(\theta, v, \omega, t)$, which gives at time t and for each ω the fraction of oscillators with phase θ and angular velocity v . The time evolution of $F(\theta, v, \omega, t)$ follows a kinetic equation, of which the incoherent state $f^0(\theta, v, \omega)$ (associated with $R_{\text{st}} = 0$) represents a stationary solution. We rewrite the kinetic equation in the form of a delay differential equation (DDE) [27, 28] for perturbations $f_t(\varphi) \equiv F(\theta, v, \omega, t + \phi)$; $-\tau \leq \phi < 0$ around $f^0(\theta, v, \omega)$. The DDE involves a linear evolution operator \mathcal{D} and a nonlinear one, \mathcal{F} . We obtain the eigenvalues and the eigenvectors of \mathcal{D} and of the corresponding adjoint operator \mathcal{D}^\dagger . As is well known [19], the knowledge of the eigenvalues allows to locate the critical value K_c of the coupling K above which the incoherent state $f^0(\theta, v, \omega)$ becomes linearly unstable. We then build for $K > K_c$ the unstable manifold expansion of the perturbation $f_t(\varphi)$ along the two complex conjugated eigenvectors associated with the instability. Using a convenient Fourier expansion of the relevant quantities and working at K slightly greater than K_c , we thus obtain the amplitude dynamics describing the evolution of perturbations $f_t(\varphi)$ in the regime of weak linear instability, $K \rightarrow K_c^+$. The nature of the amplitude dynamics at once dictates the nature of bifurcation occurring as soon as K is increased beyond K_c : The amplitude dynamics has a leading linear term and a nonlinear (cubic) term, and as is well known from the theory of bifurcation [19], the sign of the real part of this cubic term (denoted c_3 in Fig. 2) dictates the nature of the bifurcation, with positive and negative signs leading respectively to subcritical and supercritical bifurcation.

The paper is organized as follows. Section II forms the core of the paper, in which we derive our main results, Eqs. (18) and (21), with most technical details of the computation relegated to the four appendices. We illustrate our analytical results with the representative example of a unimodal Lorentzian distribution. In Section III, we make a detailed comparison of our analytical results obtained in the limit $N \rightarrow \infty$ with numerical results for finite N obtained by performing numerical integration of the equations of motion. Here, in particular, we discuss the subtleties involved in making such a comparison whose origin may be traced to finite-size effects prevalent for finite N . The paper ends with conclusions.

II. EXACT ANALYSIS IN THE LIMIT $N \rightarrow \infty$

We now turn to a derivation of our results for the system (5). To this end, consider the system in the limit $N \rightarrow \infty$, when the dynamics may be effectively characterized in terms of the single-oscillator probability density $F(\theta, v, \omega, t)$ defined above. This density is 2π -periodic in θ , and obeys the normalization

$$\int_0^{2\pi} d\theta \int_{-\infty}^{\infty} dv F(\theta, v, \omega, t) = g(\omega) \quad \forall \omega, t. \quad (13)$$

The time evolution of $F(t) \equiv F(\theta, v, \omega, t)$ may be derived by following the procedure given in Ref. [7]. One obtains the evolution equation

$$\frac{\partial F}{\partial t}(t) + v \frac{\partial F}{\partial \omega}(t) + \frac{K}{2im} (R_1[F](t - \tau) e^{-i(\theta + \alpha)} - R_{-1}[F](t - \tau) e^{i(\theta + \alpha)}) \frac{\partial F}{\partial v}(t) - \frac{1}{m} \frac{\partial}{\partial v} ((v - \omega)F(t)) = 0, \quad (14)$$

where we have defined as functionals of F the quantity

$$R_k[F] \equiv \int_0^{2\pi} d\theta \int_{-\infty}^{\infty} dv \int d\omega e^{ik\theta} F(\theta, v, \omega, t); \quad k = 0, \pm 1, \pm 2, \dots \quad (15)$$

In particular, R_{-1} coincides with the $N \rightarrow \infty$ limit of the Kuramoto order parameter (3).

From Eq. (14), one may check that the incoherent state

$$f^0(\theta, v, \omega) = g(\omega) \frac{\delta(v - \omega)}{2\pi} \quad (16)$$

solves the equation in the stationary state and thus represents an incoherent stationary state. To examine how in the stationary state the incoherent stable becomes unstable as K is tuned above a critical value K_c , we employ an unstable manifold expansion of perturbations about the incoherent state in the vicinity of the bifurcation. To perform the analysis, we write $F = f^0 + f$, with f being the perturbation, and rewrite Eq. (14) as a sum of a part \mathcal{D} linear in f and a nonlinear part \mathcal{F} :

$$\frac{\partial f_t}{\partial t} = \mathcal{D}f_t + \mathcal{F}[f_t]. \quad (17)$$

Here, we have defined $f_t(\phi) \equiv f(t + \phi)$, while the expressions of the two operators \mathcal{D} and \mathcal{F} are given in Appendix VIA. Starting with Eq. (17), the unstable manifold expansion involves a linear and a weakly nonlinear analysis, and requires combining two formalisms: i) the one developed in Ref. [18] for the case of the Kuramoto model with inertia but with no delay, ii) the delay formalism [27–29], as done in Ref. [22]. The steps are detailed in the Appendices. We summarize here the main results.

The linear stability analysis yields the dispersion relation (see Appendix VIC)

$$\Lambda(\lambda) \equiv 1 - \frac{K}{2m} e^{i(\alpha - \omega_0 \tau)} e^{-\lambda \tau} \int \frac{g(\omega + \omega_0)}{(\lambda + i\omega)(\lambda + \gamma/m + i\omega)} d\omega = 0, \quad (18)$$

which has its roots giving the eigenvalues associated with the linear operator \mathcal{D} . In particular, for $K \geq K_c$, the stationary state f^0 becomes unstable, with associated unstable eigenvalues λ satisfying $\text{Re}(\lambda) \geq 0$. Note that for $K < K_c$, the incoherent state is neutrally stable, i.e., there is no discrete eigenvalue but only a continuous spectrum; in this case, perturbations f^0 are damped in time via a mechanism similar to the Landau damping [30].

The weakly nonlinear analysis describes the type of bifurcation as $K \rightarrow K_c^+$ and hence as $\text{Re}(\lambda) \rightarrow 0^+$. The analysis involves decomposing the perturbation into a contribution along the unstable eigenvectors $P(\theta, v, \omega, \phi)$, $P^*(\theta, v, \omega, \phi)$ associated with the unstable eigenvalues λ , λ^* and a contribution $S_t(\theta, v, \omega, \phi)$ in the perpendicular direction, as

$$f_t(\phi) = (A(t)P(\phi) + \text{c.c.}) + S_t(\phi), \quad (19)$$

where c.c. stands for complex conjugation, $A(t) = (Q, f_t)_\tau$ is the amplitude of the unstable mode, and $(Q, S_t)_\tau = 0$. Here, we have introduced the eigenvector Q of the adjoint operator \mathcal{D}^\dagger and the scalar product $(\cdot, \cdot)_\tau$, see Appendix VIB.

The unstable manifold approach consists in expanding the perpendicular component S_t in terms of the small amplitude A , $S_t(\theta, v, \omega, \phi) = H[A, A^*](\theta, v, \omega, \phi)$ and computing H perturbatively. For small A (that is, in the close vicinity of K_c), it can be shown that $R(t) = A^*(t) + O(|A|^2 A^*(t))$, so that studying the bifurcation of A is equivalent

to that of the order parameter R . Following the nonlinear study based on ideas developed in Refs. [18, 22] and detailed in Appendix VID, we find the following reduced equation for the order parameter:

$$\begin{aligned} \dot{A} &= \lambda A + c_3(\lambda)|A|^2 A + O(|A|^4 A), \\ c_3(\lambda) &\sim \pi m \frac{K^3}{8\gamma^4} \frac{e^{i(\alpha - (\omega_0 + \lambda_i)\tau)}}{\Lambda'(i\lambda_i)} \frac{g(\omega_0 - \lambda_i)}{\lambda_r}, \quad \lambda_r \rightarrow 0^+, \end{aligned} \quad (20)$$

$$(21)$$

where the unstable eigenvalue λ is decomposed into its real and imaginary parts: $\lambda = \lambda_r + i\lambda_i$. A few remarks are in order: a) The coefficient c_3 diverges as $\lambda_r \rightarrow 0$, which is the regime where the reduction is valid. This singular behavior is typical of this type of systems [16, 18, 31], and stems from the existence of the continuous eigenspectrum that cannot be described by the finite dimensional equation (20). b) However, we still expect the behavior of c_3 to determine the type of bifurcation. For $\text{Re}(c_3) > 0$, we expect a subcritical (discontinuous) bifurcation, while for $\text{Re}(c_3) < 0$, we expect a supercritical bifurcation. In the latter case, the scaling of the stationary amplitude is $A_{\text{st}} \propto \lambda_r$, which differs from the usual Kuramoto model where it goes as $\sqrt{\lambda_r}$. c) In the case with no inertia, that is, with $m = 0$, we expect the coefficient c_3 to be quantitatively relevant in giving the exact amplitude A_{st} of the stationary branch close to the bifurcation; here, because of the singularity, only the sign and scaling of $c_3(\lambda)$ can be used to get qualitative information.

A. Application to a Lorentzian distribution

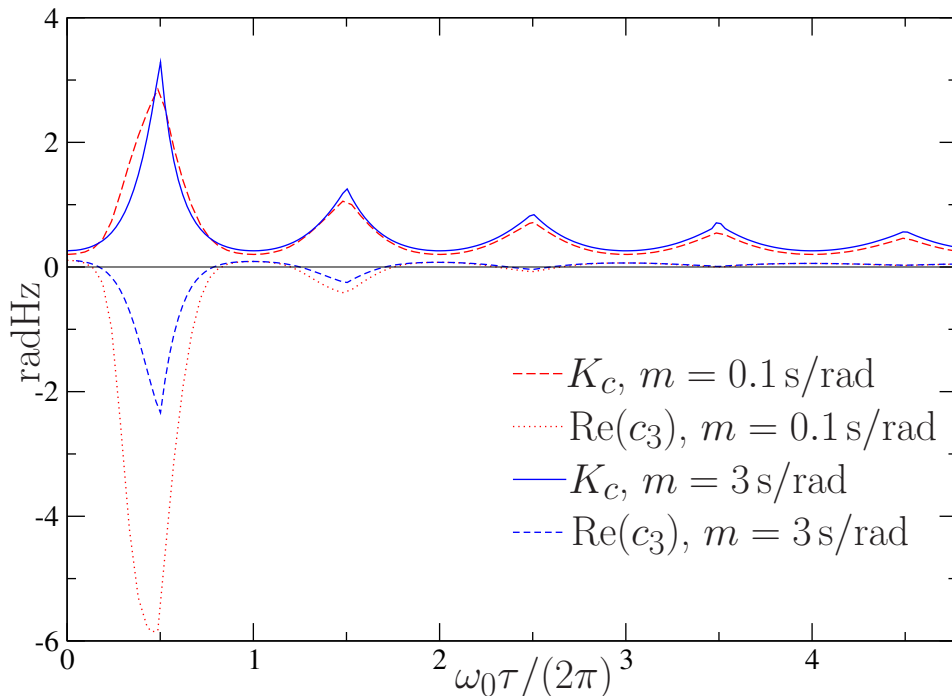


FIG. 2: Stability region of the incoherent state for Lorentzian $g_L(\omega) = \sigma/[\pi((\omega - \omega_0)^2 + \sigma^2)]$ with $\sigma = 0.1$ radHz and $\omega_0 = 3$ radHz. We show here as a function of τ the quantities $K_c(\tau)$ and $\text{Re}(c_3)(\tau)$ for $m = 0.1$ s/rad and $m = 3$ s/rad. The sign of $\text{Re}(c_3)(\tau)$ determines the super/sub-critical nature of the bifurcation.

To assess the effects of inertia in a delay system, we consider a Lorentzian distribution of the natural frequencies: $g_L(\omega) = \sigma/[\pi((\omega - \omega_0)^2 + \sigma^2)]$. The dispersion relation (18) at criticality gives $K = K_c$ and $\lambda = 0^+ + i\lambda_{i,c}$:

$$\frac{K_c}{2} = (\gamma\sigma + m\sigma^2 - m\lambda_{i,c}^2) \csc((\omega_0 + \lambda_{i,c})\tau), \quad (22)$$

$$\frac{\lambda_{i,c}(\gamma + 2\sigma m)}{\gamma\sigma + m\sigma^2 - m\lambda_{i,c}^2} = -\tan((\omega_0 + \lambda_{i,c})\tau). \quad (23)$$

Solving this system gives us $K_c(\tau)$ and $\lambda_{i,c}(\tau)$. Then the sign of the cubic coefficient $\text{Re}(c_3)(\tau)$ is given by

$$s(\tau) = \text{Re} \left(\frac{(\sigma + i\lambda_{i,c})^2 (\gamma + m(\sigma + i\lambda_{i,c}))^2}{m(\gamma + (\sigma + i\lambda_{i,c})(\gamma\tau + m(i\lambda_{i,c}\tau + \sigma\tau + 2)))} \right), \quad (24)$$

where we used Eq. (21) with $g = g_L$. We plot in Fig. 2 the quantities K_c and $\text{Re}(c_3)$ as a function of the delay for two different inertia values $m = 0.1$ and $m = 3 \text{ s/rad}$ for a Lorentzian distribution. For $\tau \rightarrow 0$, we recover the no-delay results showing a positive $\text{Re}(c_3)$ and hence a subcritical bifurcation [7]. Moreover, as in the case with no inertia [22], $m = 0$, the delay induces “oscillations” in the sign of $\text{Re}(c_3)$. We observe that different nonzero values of m do not change much the behavior of the bifurcation.

III. NUMERICAL RESULTS

A. Method

In the preceding section, we provided an analytic characterization of the stability properties of the incoherent state in the Kuramoto model with delayed coupling and inertia in the limit $N \rightarrow \infty$. Here we present results from numerical integration of the dynamics (5) with Lorentzian-distributed natural frequencies with location parameter $\omega_0 = 3 \text{ radHz}$ and scale parameter $\sigma = 0.1 \text{ radHz}$. For all-to-all coupling, Eq. (5) can be rewritten in terms of the Kuramoto order parameter: Using $R_x(t - \tau) = 1/N \sum_j \cos(\theta_j(t - \tau))$ and $R_y(t - \tau) = 1/N \sum_j \sin(\theta_j(t - \tau))$, we rewrite the equations of motion as

$$\dot{\theta}_i(t) = v_i(t), \quad (25)$$

$$m\dot{v}_i(t) + \gamma v_i(t) = \gamma\omega_i + K [R_y(t - \tau) \cos(\theta_i(t)) - R_x(t - \tau) \sin(\theta_i(t))].$$

As mentioned earlier, the effect of α for a fixed τ can be studied by considering $\alpha - \omega_0\tau$ instead of τ in the dynamics, hence here we have set α to zero without loss of generality. Hence, for $\gamma = 1$, we have the set of equations

$$\dot{\theta}_i(t) = \omega_i + K x_i^C(t), \quad (26)$$

$$\dot{x}_i^C(t) = \frac{1}{m} (x_i^{\text{PD}}(t) - x_i^C(t)), \quad (27)$$

$$x_i^{\text{PD}}(t) = R_y(t - \tau) \cos(\theta_i(t)) - R_x(t - \tau) \sin(\theta_i(t)), \quad (28)$$

which we integrate numerically using an Euler iteration-method, given the initial phases $\theta_i(0)$ independently and identically distributed in $[0, 2\pi)$, and initial state of the filters $x_i^C(0)$. $R_x(t_{\text{hist}})$ and $R_y(t_{\text{hist}})$ with $t_{\text{hist}} \in [-\tau, 0]$ are given by the history of the network of oscillators, which we obtain by evolving each oscillator independently according to its own natural frequency. The code is written in python and compiled with cython for fast execution and can be found on the Gitlab repository here [32].

Our objective behind performing the numerics is to verify our theoretical results obtained in the thermodynamic limit for the critical coupling constant K_c above which the incoherent state becomes unstable. Furthermore, we want to confirm the type of bifurcation as predicted by our theoretical results that can be observed as the coupling constant K is tuned across K_c . To this end, we integrate numerically the dynamics of large networks of all-to-all delay-coupled PLL clocks in the vicinity of the theoretically-predicted K_c , see Fig. 2.

We proceed with our numerical work as follows. For a given set of parameters $(N, \tau, m, \gamma = 1, \alpha = 0)$, a vector of discrete coupling constants $K_n = \{K_{\text{on}}, K_{\text{on}} + \Delta K, \dots, K_{\text{end}} - \Delta K, K_{\text{end}}\}$; $\Delta K > 0$ and a set of Lorentzian-distributed natural frequencies $\{\omega_i\}$, each oscillator is evolved independently with its own natural frequency for a time τ to obtain the dynamical history for N PLLs in the interval $[-\tau, 0]$. In the next step, we turn on the coupling between the oscillators at an initial coupling constant K_{on} that is close to but smaller than the critical coupling constant predicted by our theoretical results. Subsequently, the delay-coupled system of all-to-all coupled PLLs is evolved with the coupling constant kept fixed at K_{on} for time T_{num} that is long compared to the mean period of the independent oscillators, in order to ensure that the system settles into a stationary state at the fixed value of the coupling. Then, using the phases of the final interval $[T_{\text{num}} - \tau, T_{\text{sim}}]$ as the history, we evolve the system of coupled oscillators for the next larger value in K_n for time T_{num} , and so on, until the value K_{end} is reached. In the final part of this procedure, we follow the exact reverse protocol, namely, repeating the above steps while decreasing the value of the coupling from K_{end} until the value $K_{\text{on}} < K_c$ is reached. In numerics, we track the value of the Kuramoto order parameter in time, and save for each value of the coupling in the set K_n the final value of the order parameter obtained at the end of run for time T_{num} as well as its average and variance computed over a time equal to 50 times the time period corresponding to ω_0 .

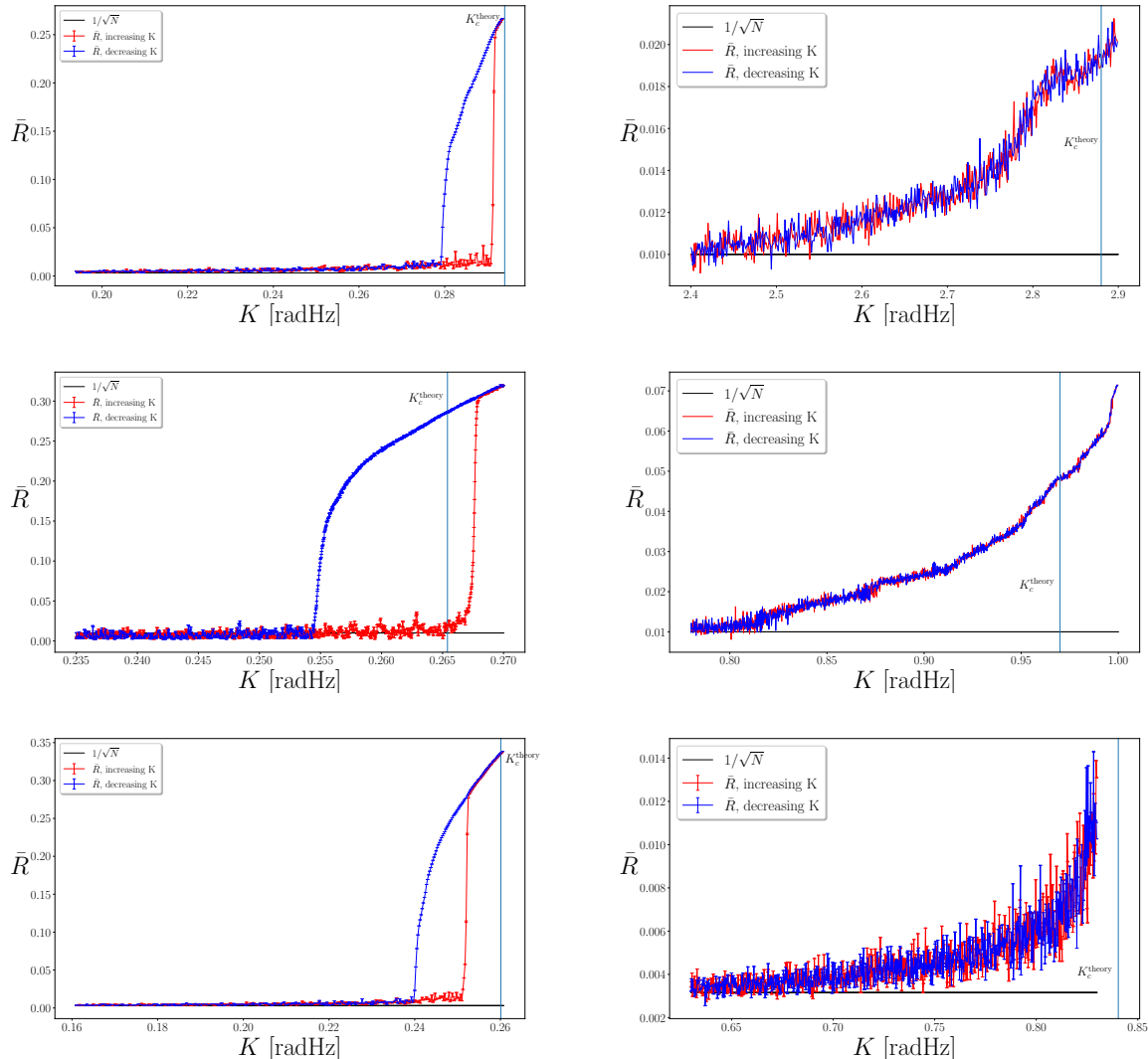


FIG. 3: Numerical integration results for the average Kuramoto order-parameter $\bar{R}(t)$ as a function of the coupling constant K in the vicinity of the critical coupling constant K_c . Plots show the cases with inertia $m = 3.0$ s/rad and $\tau = \{0.2, 1.0, 2.0, 3.0, 4.2, 5.25\}$ s starting in the upper left corner and continuing to the right and downwards. For each value of K , the system of $N = 10^5$ oscillators was integrated for $T_{\text{num}} = 2500$ s, and the K -values are separated by $\Delta K = (2.5 \times 10^{-4})/(2\pi)$ Hz, see text.

B. Results

We present in Figs. 3 and 4 results for transmission delays $\tau = \{0.2, 1.0, 2.0, 3.0, 4.2\}$ s and moments of inertia $m = \{0.1, 3.0\}$ s/rad, obtained for a system of $N = 100000$ all-to-all coupled oscillators. In both the figures, the left panels (respectively, right panels) show the cases for which the theory predicts $\text{Re}(c_3) > 0$ and hence a subcritical bifurcation and presence of a hysteresis loop (respectively, $\text{Re}(c_3) < 0$ and hence a supercritical bifurcation with no hysteresis). The plots show the Kuramoto order parameter averaged over a time equal to 50 times the time period corresponding to the frequency ω_0 and plotted as a function of the coupling constant K .

In our simulations we find the bifurcations that were predicted by the theoretical results. As the coupling constant K increases, it crosses a critical coupling constant K_c^{num} as found in our finite-size simulation, and we observe a subcritical (discontinuous) transition and hysteresis for $\text{Re}(c_3) > 0$. For $\text{Re}(c_3) < 0$ on the other hand, we find a supercritical (continuous) transition with a linearly growing order parameter and no hysteresis as K grows larger than K_c^{num} . We observe that for the case of $m = 0.1$ s/rad, the hysteresis seems to be weaker than in the case with

$m = 3.0$ s/rad. The results are in good agreement with our theoretical predictions for K_c and the type of bifurcation.

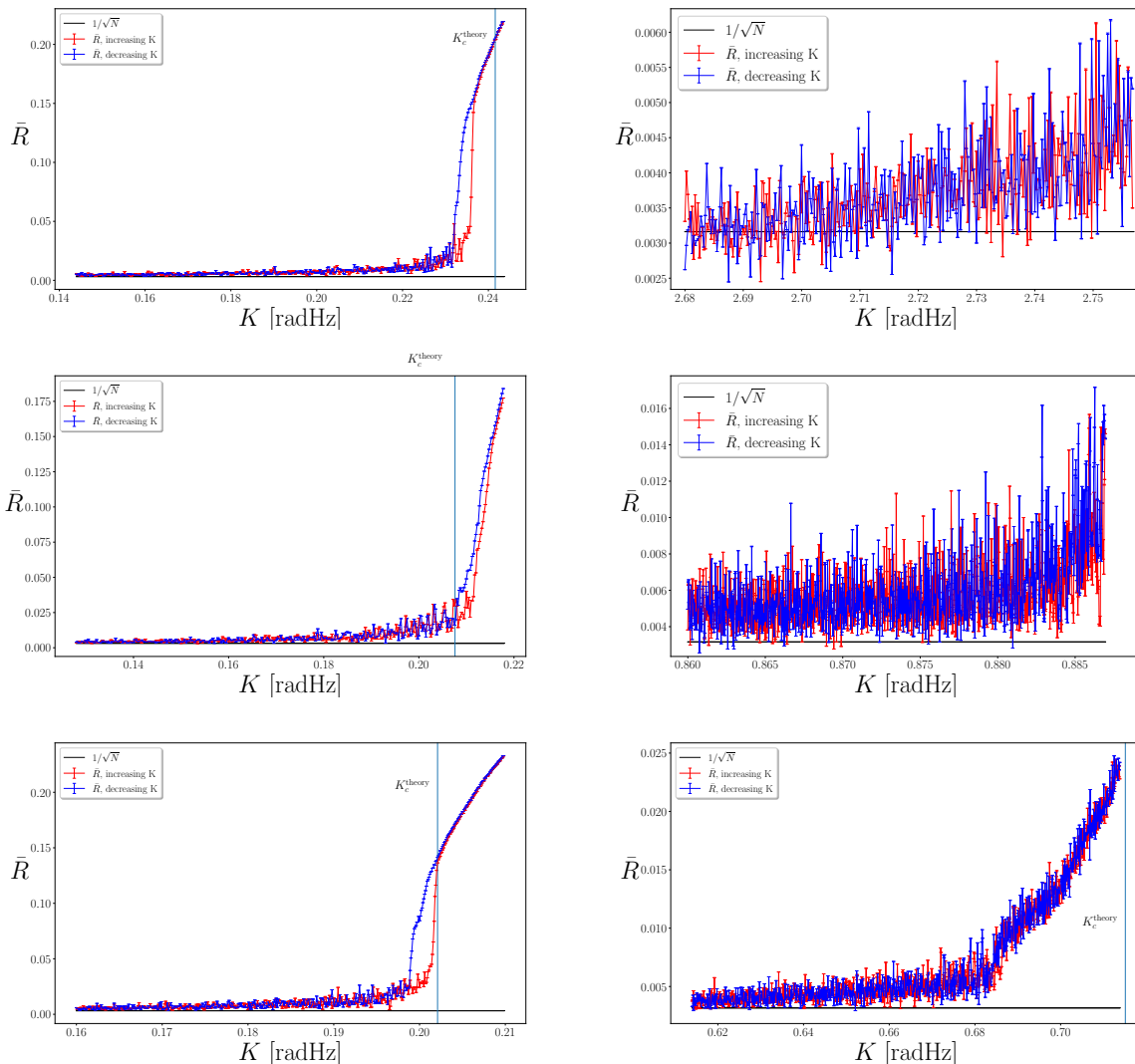


FIG. 4: Numerical integration results as in Fig. 3 but for $m = 0.1$ s/rad.

C. Discussion of numerical results

Numerical validation of our analytical results obtained in the thermodynamic limit is not trivial and comes with a few difficulties that we will discuss here. Since we do not know the system size N_{crit} of oscillators below which strong finite-size effects will come into play and the number N_{thermo} above which the behavior coincides with that in the thermodynamic limit, we decided while doing our numerical checks to go for as large a system size as is practicable. This however becomes very resource intensive, since for systems with time delays, a memory of the states of all oscillators for a time period $[t - \tau, t]$ has to be stored in order to perform dynamical evolution. For the mean-field coupling case, we have the advantage that it is sufficient to keep only the history of the order parameter variables $R_x(t - \tau)$ and $R_y(t - \tau)$.

It is known from the literature [33] that for the Kuramoto model in absence of delay and inertia, when the number of oscillators is finite, we may expect to find $K_c^{\text{num}} \leq K_c^{\text{theory}}$, depending on the number N of oscillators considered. This difference is even stronger when considering the inertial model and subcritical bifurcation, where the convergence

$K_c^{\text{theory}}(N) - K_c^{\text{num}}(N) \sim N^{-0.22}$ [17] is very slow with N (compared with $K_c^{\text{theory}}(N) - K_c^{\text{num}}(N) \sim N^{-0.4}$ without inertia [33]). Note that the prediction $K_c^{\text{theory}} > K_c^{\text{num}}$ was obtained for systems without delay, thus observing $K_c^{\text{theory}} \approx K_c^{\text{num}}$ in Fig. 3 and Fig. 4 at $\tau = 2$ s does not contradict the results in [17, 33] and raises an interesting issue for future investigation as to how the difference between K_c^{num} and K_c^{theory} scales with N . However, in cases with supercritical bifurcation, the numerically observed value of the critical coupling seems more different from the theoretical value than in cases with subcritical bifurcation (which could be another indicator of the type of transition). We thus have no prior knowledge of the exact value $K_c^{\text{num}}(N)$ at which to expect the transition. Furthermore, the multistability present in the system due to the delayed interaction results in a number of step-like transitions that follow once the incoherent state becomes unstable. As a consequence, validation of a linear and continuous transition for $K > K_c$ becomes hard to resolve when increasing K_n further than the regime of the continuous transition. For smaller values of the inertia, the discontinuous transitions and hysteresis regimes also become much smaller, and it becomes difficult to resolve them even with, e.g., $N = 10^5$ oscillators. Furthermore, there are no a priori conditions to guide us while choosing the values of ΔK and T_{sim} . The tests required in estimating the right choices for the dynamical parameters are computationally expensive and require long computation times.

IV. CONCLUSIONS

In this work, we have studied the effect of time delay in the interaction between oscillators within the framework of the inertial Kuramoto model of globally coupled oscillators. For a generic choice of the natural frequency distribution of the oscillators, we obtain exact analytical results that imply that in contrast to the case with no delay, the system in the stationary state may exhibit either a subcritical or a supercritical bifurcation between a synchronized and an incoherent phase. The precise nature of bifurcation has an essential dependence on the amount of delay present in the interaction as also on the value of inertia of the oscillators. Our theoretical analysis, performed in the limit of an infinite number of oscillators, is carried out by employing an unstable manifold expansion in the vicinity of the bifurcation, which we apply to the kinetic equation satisfied by the single-oscillator distribution function, Eq. (14). The one-dimensional reduction, Eq. (20), of the dynamics for the order parameter is plagued by singularities that are reminiscent of an infinite dimensional bifurcation and, thus, gives at best qualitative information on the bifurcation nature, a fact that our numerical results fully support. We notice, however, that the unstable manifold method is very robust in the context of kinetic equations with continuous spectrum, since it is, to the best of the authors' knowledge, the only one giving analytic predictions for the Kuramoto model both with inertia $m \neq 0$ and delay $\tau \neq 0$, while other methods, like the Ott-Antonsen ansatz [34], work only for $m = 0$, while self-consistent methods e.g. [1] have been applied only for the case with no delay, $\tau = 0$. Direct numerical integration of the dynamics allows to highlight the subtleties one is confronted with when checking the analytical results against those obtained numerically for a finite number of oscillators. For systems of delay-coupled PLLs with heterogeneous natural frequencies, our results allow to predict the minimal coupling sensitivity of the voltage-controlled oscillators necessary to enable the network to become synchronized. Moreover, such PLL networks generally seem to exit the incoherent state at smaller coupling sensitivity if the transition happens through a subcritical bifurcation, $\text{Re}(c_3) > 0$, and close to integer multiples of the mean natural period of the oscillators, where we find the local minima of K_c , see Fig. 2. It may be noted that with increasing transmission delay, the onset of synchronization can generally be achieved at smaller values of K_c . Hence, larger values of the transmission delay seem to decrease the stability of the incoherent state.

V. ACKNOWLEDGEMENTS

This work was done during SG's visit to the Max Planck Institute for the Physics of Complex Systems, Dresden, Germany during November 2016 and September 2018 and his visit to the International Centre for Theoretical Physics, Trieste, Italy (as a Regular Associate of the Quantitative Life Sciences Section) and Sapienza Università di Roma, Rome, Italy during May-June 2019. He thanks these organizations as well as his parent organization, Ramakrishna Mission Vivekananda Educational and Research Institute, for supporting his visits. DM gratefully acknowledges the support of the U.S. Department of Energy through the LANL/LDRD Program and the Center for Non Linear Studies, LANL.

VI. APPENDIX

A. Theory of delay differential equations

The time evolution of a function $F(t)$ according to a nonlinear operator with delay, $M[F(t)]$, can be rewritten in term of a delay variable φ such that the time-evolution operator is given by

$$(\mathcal{A}F_t)(\varphi) = \begin{cases} \frac{d}{d\varphi}F_t(\varphi), & -\tau \leq \varphi \leq 0, \\ M[F_t], & \varphi = 0, \end{cases} \quad (29)$$

with $F_t(\phi) \equiv F(t + \phi)$. Expanding around a stationary state f^0 , as $F = f^0 + f$, with f being a perturbation, we define the linear and nonlinear operators \mathcal{D} and \mathcal{F} , according to

$$(\mathcal{A}f_t)(\varphi) = (\mathcal{D}f_t + \mathcal{F}[f_t])(\varphi) = \begin{cases} \frac{d}{d\varphi}f_t(\varphi) \\ \mathcal{L}f_t(\varphi) \end{cases} + \begin{cases} 0, & -\tau \leq \varphi < 0, \\ \mathcal{N}[f_t], & \varphi = 0. \end{cases} \quad (30)$$

We decompose the linear operator into two parts, $\mathcal{L} = \mathbf{L} + \mathbf{R}$, namely, a part \mathbf{L} that does not contain any delay term and a part \mathbf{R} that has all the delay terms. Rewriting Eq. (14) according to the above formalism yields

$$\frac{\partial f_t}{\partial t} = \mathcal{D}f_t + \mathcal{F}[f_t], \quad (31)$$

with

$$\mathbf{L}f = -v\partial_\theta f + \frac{1}{m}\partial_v((v - \omega)f), \quad (32)$$

$$\mathbf{R}f = -\frac{K}{2im} \left(R_1[f]e^{-i\theta}e^{-i(\alpha - \omega_0\tau)} - R_{-1}[f]e^{i\theta}e^{i(\alpha - \omega_0\tau)} \right) \partial_v f^0, \quad (33)$$

$$\mathcal{N}[f_t] = -\frac{K}{2im} \left(R_1[f_t](-\tau)e^{-i\theta}e^{-i\alpha} - R_{-1}[f_t](-\tau)e^{i\theta}e^{i\alpha} \right) \partial_v f(0), \quad (34)$$

where we use the shorthand $\partial_v \equiv \partial/\partial v$ for derivatives and use in all appendices the transformation $m \rightarrow m/\gamma$ and $K \rightarrow K/\gamma$. Moreover, to simplify the Appendices, we work in the rotating frame $\theta_j(t) \rightarrow \theta_j(t) - \omega_0 t$, $\omega_j \rightarrow \omega_j - \omega_0 \forall j$, so that the distribution $g(\omega)$ is now centerer in 0.

B. Dual space

In the functional space of delayed functions, there is no \mathcal{L}_2 canonical inner product. However, Ref. [27] defines a bilinear form acting as the inner product on this space. In our problem with a discrete delay, the scalar product is

$$(q, p)_\tau \equiv (q(0), p(0)) + \int_{-\tau}^0 d\xi (q(\xi + \tau), \mathbf{R}p(\xi)), \quad (35)$$

where $(q(0), p(0))$ denotes the usual scalar product on $\mathcal{L}_2(\mathbb{T} \times \mathbb{R} \times \mathbb{R})$ (phase, angular velocity and natural frequency)

$$(h, f) = \int_{\mathbb{T} \times \mathbb{R} \times \mathbb{R}} h^*(\theta, v, \omega) f(\theta, v, \omega) d\omega dv d\theta, \quad \text{with } q(0) = h(\theta, v, \omega), \quad p(0) = f(\theta, v, \omega) \quad (36)$$

and the integral term contains the delay contribution. The adjoint of the linear operator \mathcal{D} , obtained by using the equality $(q(\varphi), \mathcal{D}p(\varphi))_\tau = (\mathcal{D}^\dagger q(\varphi), p(\varphi))_\tau$, is defined in the dual space, and is given by

$$(\mathcal{D}^\dagger q_t)(\vartheta) = \begin{cases} -\frac{d}{d\vartheta}q_t(\vartheta), & 0 < \vartheta \leq \tau, \\ \mathcal{L}^\dagger q_t(\vartheta), & \vartheta = 0. \end{cases} \quad (37)$$

We also decompose $\mathcal{L}^\dagger = \mathbf{L}^\dagger + \mathbf{R}^\dagger$, with

$$\mathbf{L}^\dagger q = v\partial_\theta q - \frac{1}{m}(v - \omega)\partial_v q, \quad (38)$$

$$\mathbf{R}^\dagger q = \frac{K}{2im} \left(e^{i\alpha}e^{-i\theta} R_1[q\partial_v f^0] - e^{-i\alpha}e^{i\theta} R_{-1}[q\partial_v f^0] \right). \quad (39)$$

C. Eigenvalue problem

We now solve the eigenvalue problem

$$(\mathcal{D}P)(\varphi) = \lambda P(\varphi) \quad (40)$$

for $-\tau \leq \varphi < 0$; we get for $\varphi \neq 0$, $P(\varphi) = \Psi e^{\lambda\varphi}$ for arbitrary Ψ . We expand in a Fourier series in θ , as $P(\varphi) = (2\pi)^{-1} \sum_{k=-\infty}^{\infty} p_k(\varphi) e^{ik\theta}$ and $\Psi(\theta, \omega) = (2\pi)^{-1} \sum_{k=-\infty}^{\infty} \psi_k(\omega) e^{ik\theta}$. Using Eq. (40) for $\varphi = 0$ and $k = \pm 1$ in the Fourier expansion, we get

$$p_1(\varphi) = \psi_1(\omega, v) e^{i\theta + \lambda\varphi}. \quad (41)$$

In the following, we will omit subscripts while referring to ψ_1 and p_1 . For $\varphi = 0$, we look for a solution of the eigenvalue problem in the form

$$\psi = U_0(\omega) \delta(v - \omega) + U_1(\omega) \delta'(v - \omega), \quad (42)$$

where the Dirac delta function and its derivatives are to be understood in the distribution sense. Imposing the normalization $R_1[\Psi] = R_{-1}[\Psi] = \int dv d\omega \psi = 1$, one finds

$$U_0 = \frac{K}{2m} e^{i(\alpha - \omega_0\tau)} e^{-\lambda\tau} \frac{g(\omega)}{(\lambda + i\omega)(\lambda + 1/m + i\omega)}, \quad (43)$$

$$U_1 = \frac{K}{2im} e^{i(\alpha - \omega_0\tau)} e^{-\lambda\tau} \frac{g(\omega)}{\lambda + 1/m + i\omega}. \quad (44)$$

Expliciting the normalization condition yields the dispersion relation:

$$\Lambda(\lambda) = 1 - \frac{K}{2m} e^{i(\alpha - \omega_0\tau)} e^{-\lambda\tau} \int d\omega \frac{g(\omega)}{(\lambda + i\omega)(\lambda + 1/m + i\omega)} = 0. \quad (45)$$

We can see that $p^*(\varphi)$ gives another eigenfunction of \mathcal{D} with eigenvalues λ^* , so that $\Lambda(\lambda) = \Lambda^*(\lambda^*) = 0$. For $k \neq \pm 1$, one has only a continuous spectrum occupying the imaginary axis.

The adjoint eigenvector has the form $Q(\vartheta) = \tilde{\Psi} e^{-\lambda^*\vartheta} = \tilde{\psi} e^{i\theta} e^{-\lambda^*\vartheta}$, where $\tilde{\psi}$ solves

$$(\lambda^* - iv)\tilde{\psi} + \frac{1}{m}(v - \omega)\partial_v \tilde{\psi} = \frac{K}{2im} e^{-i(\alpha - \omega_0\tau)} e^{-\lambda^*\tau} \int d\omega g(\omega) \partial_v \tilde{\psi}(\omega, \omega). \quad (46)$$

Full solution of the above equation is not straightforward to obtain, but thankfully we just need to know $\tilde{\psi}(\omega, \omega)$ and the derivative $\tilde{\psi}^{(n)}(\omega) = \partial_v^n \tilde{\psi}(\omega, \omega)$, which may be obtained by successive differentiation of Eq. (46).

D. Unstable manifold Expansion

To perform the weakly nonlinear analysis, we will expand the perturbation $f_t(\phi)$ along the unstable eigenvector and the unstable manifold. The decomposition on the unstable manifold reads

$$f_t(\varphi) = A(t)P(\varphi) + A^*(t)P^*(\varphi) + H[A, A^*](\varphi), \quad (47)$$

with $A(t) = (Q, f_t)_\tau$, $(Q, P^*) = 0$ and $(Q, H) = 0$. We assume that H is at least of order $(A, A^*)^2$. The amplitude A is directly related to the Kuramoto order parameter R as $R = A^* + O(|A|^2 A^*)$. Let us define the following Fourier expansions needed for further analysis:

$$f_t = \frac{1}{2\pi} \sum_{k=-\infty}^{\infty} (f_t)_k e^{ik\theta}, \quad (48)$$

$$\{\mathcal{L} f_t, \mathcal{N}[f_t]\} = \frac{1}{2\pi} \sum_{k=-\infty}^{\infty} \{\mathcal{L}_k (f_t)_k, \mathcal{N}_k[f_t]\} e^{ik\theta}, \quad (49)$$

$$H[A, A^*] = \frac{1}{2\pi} |A|^2 w_0 [|A|^2] + \frac{1}{2\pi} \sum_{k=1}^{\infty} (A^k w_k [|A|^2] e^{ik\theta} + (A^*)^k w_{-k} [|A|^2] e^{-ik\theta}), \quad (50)$$

where the dependance on A of the Fourier coefficients of H is imposed by rotational symmetry [31]. To proceed with the analysis, we will need to expand the coefficients w_k in powers of $|A|^2$, $w_k = \sum_{j=0}^{\infty} |A|^{2j} w_{k,j}$. To be consistent with the assumption of the unstable manifold being at least of order $(A, A^*)^2$, we need to have $w_{\pm 1,0} = 0$.

The Fourier coefficients of the nonlinear operator (34) are

$$\mathcal{N}_k[f_t] = \frac{iK}{2m} \left(e^{-i\alpha} R_1[f_t](-\tau) \partial_v (f_t)_{k+1}(0) - e^{i\alpha} R_{-1}[f_t](-\tau) \partial_v (f_t)_{k-1}(0) \right). \quad (51)$$

Note that contrary to the case with no inertia, $m = 0$, where $\mathcal{L}_0 = \mathcal{N}_0 = 0$ so that $(f_t)_0 = \text{constant} = 0$, it is not so in the present case so that $(f_t)_0 \neq 0$ and $w_0 \neq 0$. This difference will have major consequences for the reduction, like a $1/\lambda$ divergence in the c_3 coefficient.

For $\varphi \neq 0$, we find $w_0(\varphi) = h_{0,0} e^{2\lambda_r \varphi} + O(|A|^2)$, $w_{2,0}(\varphi) = h_{2,0} e^{2\lambda \varphi} + O(|A|^2)$, and with the boundary equation $\varphi = 0$:

$$(2\lambda_r - \mathcal{L}_0) \cdot h_{0,0} = i \frac{K}{2m} e^{-i(\alpha - \omega_0 \tau)} e^{-\lambda^* \tau} \partial_v \psi + \text{c.c.}, \quad (52)$$

$$(2\lambda - \mathcal{L}_2) \cdot h_{2,0} = -i \frac{K}{2m} e^{i(\alpha - \omega_0 \tau)} e^{-\lambda \tau} \partial_v \psi. \quad (53)$$

Solving these equation will give us $h_{0,0}$ and $h_{2,0}$ needed in the following. Projection of the dynamics along the unstable mode using $(Q, (31))_\tau$ yields the equation for the amplitude $A(t)$ to be

$$\dot{A} = \lambda A + c_3 A |A|^2 + O(A |A|^4), \quad (54)$$

$$c_3 = \frac{K}{2im} \left(e^{i(\alpha - \omega_0 \tau)} e^{-\lambda \tau} \int d\omega \tilde{\psi}^* \partial_v h_{0,0} - e^{-i(\alpha - \omega_0 \tau)} e^{-\lambda^* \tau} \int d\omega \tilde{\psi}^* \partial_v h_{2,0} \right), \quad (55)$$

where we used Eq. (51) for $k = 1$ keeping only the leading order. To determine the nature of the bifurcation, we must compute explicitly the coefficient c_3 . To do that, we must first compute the Fourier component of the unstable manifold.

1. Computation of $h_{0,0}$

We start with Eq. (52). We have $h_{0,0} = h + \text{c.c.}$, where h is the solution of

$$(2\lambda_r - \mathcal{L}_0) \cdot h = i \frac{2\pi K}{2m} e^{-i(\alpha - \omega_0 \tau)} e^{-\lambda^* \tau} \partial_v \psi. \quad (56)$$

Equation (56) reads

$$2\lambda_r h_{0,0} - \frac{1}{m} \partial_v [(v - \omega) h_{0,0}] = \frac{K^2}{4im^2} e^{-2\lambda_r \tau} \left(\frac{g\delta'(v - \omega)}{(\lambda^* - i\omega)(\lambda^* - i\omega + 1/m)} + i \frac{g\delta''(v - \omega)}{(\lambda^* - i\omega + 1/m)} \right). \quad (57)$$

We introduce the ansatz

$$h = W_0(\omega) \delta(v - \omega) + W_1(\omega) \delta'(v - \omega) + W_2(\omega) \delta''(v - \omega), \quad (58)$$

to get

$$W_0(\omega) = 0, \quad (59)$$

$$W_1(\omega) = \frac{(K/2m)^2 e^{-2\lambda_r \tau} g(\omega)}{(2\lambda_r + 1/m)(\lambda + i\omega)(\lambda + 1/m + i\omega)}, \quad (60)$$

$$W_2(\omega) = \frac{(K/2m)^2 e^{-2\lambda_r \tau} g(\omega)}{2(\lambda_r + 1/m)(\lambda + 1/m + i\omega)}. \quad (61)$$

2. Computation of $h_{2,0}$

A similar computation starting from Eq. (53) yields $h_{2,0}$. We have to solve

$$(2\lambda - \mathcal{L}_2) \cdot h_{2,0} = -i \frac{K}{2m} e^{i(\alpha - \omega_0 \tau)} e^{-\lambda \tau} \partial_v \psi. \quad (62)$$

Using the ansatz

$$h_{2,0} = X_0\delta(v - \omega) + X_1\delta'(v - \omega) + X_2\delta''(v - \omega), \quad (63)$$

we obtain

$$X_0(\omega) = \frac{iX_1(\omega)}{(\lambda + i\omega)}, \quad (64)$$

$$X_1(\omega) = \frac{-i(Ke^{i(\alpha-\omega_0\tau)}e^{-\lambda\tau}/2m)U_0(\omega)}{(2\lambda + 2i\omega + 1/m)} + \frac{4iX_2(\omega)}{(2\lambda + 2i\omega + 1/m)}, \quad (65)$$

$$X_2(\omega) = \frac{-i(Ke^{i(\alpha-\omega_0\tau)}e^{-\lambda\tau}/2m)U_1(\omega)}{2(\lambda + i\omega + 1/m)}. \quad (66)$$

3. Putting everything together

One can ascertain that the only diverging term will come from $\int \tilde{\psi}^{(2)*}W_1^* d\omega$; thus, the leading term is

$$\int d\omega \tilde{\psi}^{(2)*}W_1^* \sim i \frac{K^2}{2m^2} \frac{e^{-2\lambda_r\tau}}{(1/m)^4} \frac{1}{\Lambda'(i\lambda_i)} \frac{\pi}{2} \frac{g(-\lambda_i)}{\lambda_r}. \quad (67)$$

We conclude that the leading behavior of c_3 for $m > 0$ is given by

$$c_3 \sim \frac{m\pi K^3}{8} \frac{e^{i(\alpha-(\omega_0+\lambda_i)\tau)}}{\Lambda'(i\lambda_i)} \frac{g(-\lambda_i)}{\lambda_r}. \quad (68)$$

In particular, the sign of $s(\tau) \equiv \text{Re} \left(\frac{e^{i(\alpha-(\omega_0+\lambda_i)\tau)}}{\Lambda'(i\lambda_i)} \right)$ determines the type (sub- vs. super-critical) of the bifurcation.

-
- [1] H. A. Tanaka, A. J. Lichtenberg, and S. Oishi, *First order phase transition resulting from finite inertia in coupled oscillator systems*, Phys. Rev. Lett. **78**, 2104 (1997).
- [2] A. J. Acebrón and R. Spigler, *Adaptive frequency model for phase-frequency synchronization in large populations of globally coupled nonlinear oscillators*, Phys. Rev. Lett. **81**, 2229 (1998).
- [3] J. A. Acebrón, L. L. Bonilla and R. Spigler, *Synchronization in populations of globally coupled oscillators with inertial effects*, Phys. Rev. E **62**, 3437 (2000).
- [4] Y. Kuramoto, *Chemical oscillations, waves, and turbulence* (Springer-Verlag, Berlin, 1984).
- [5] S. H. Strogatz, *From Kuramoto to Crawford: Exploring the onset of synchronization in populations of coupled oscillators*, Physica D **143**, 1 (2000).
- [6] J. A. Acebrón, L. L. Bonilla, C. J. Pérez Vicente, F. Ritort and R. Spigler, *The Kuramoto model: A simple paradigm for synchronization phenomena*, Rev. Mod. Phys. **77**, 137 (2005).
- [7] S. Gupta, A. Campa and S. Ruffo, *Kuramoto model of synchronization: Equilibrium and non-equilibrium aspects*, J. Stat. Mech.: Theory Exp. R08001 (2014).
- [8] F. A. Rodrigues, T. K. DM. Peron, P. Ji and J. Kurths, *The Kuramoto model in complex networks*, Phys. Rep. **610**, 1 (2016).
- [9] S. Gherardini, S. Gupta and S. Ruffo, *Spontaneous synchronization and nonequilibrium statistical mechanics of coupled phase oscillators*, Contemporary Physics **59**, 229 (2018).
- [10] S. Gupta, A. Campa and S. Ruffo, *Statistical physics of synchronization* (Springer-Verlag, Berlin, 2018).
- [11] J. Buck, *Synchronous rhythmic flashing of fireflies. II.*, Q. Rev. Biol. **63**, 265 (1988).
- [12] C. S. Peskin, *Mathematical aspects of heart physiology* (Courant Institute of Mathematical Sciences, New York, 1975).
- [13] S. P. Benz and C. J. Burroughs, *Coherent emission from twodimensional Josephson junction arrays*, Appl. Phys. Lett. **58**, 2162 (1991).
- [14] I. Kiss, Y. Zhai and J. Hudson, *Emerging coherence in a population of chemical oscillators*, Science **296**, 1676 (2002).
- [15] A. A. Temirbayev, Z. Zh. Zhanabaev, S. B. Tarasov, V. I. Ponomarenko and M. Rosenblum, *Experiments on oscillator ensembles with global nonlinear coupling*, Phys. Rev. E **85**, 015204(R) (2012).
- [16] J. D. Crawford, *Scaling and singularities in the entrainment of globally coupled oscillators*, Phys. Rev. Lett. **74**, 4341 (1995).
- [17] S. Olmi, A. Navas, S. Boccaletti and A. Torcini, *Hysteretic transitions in the Kuramoto model with inertia*, Phys. Rev. E **90**, 042905 (2014).

- [18] J. Barré and D. Métivier, *Bifurcations and singularities for coupled oscillators with inertia and frustration*, Phys. Rev. Lett. **117**, 214102 (2016).
- [19] S. H. Strogatz, *Nonlinear Dynamics and Chaos: with Applications to Physics, Biology, Chemistry, and Engineering* (Westview Press, Boulder, 2014).
- [20] H. Sakaguchi and Y. Kuramoto, *A soluble active rotator model showing phase transitions via mutual entrainment*, Prog. Theor. Phys. **76**, 576 (1986).
- [21] M. K. Stephen Yeung and S. H. Strogatz, *Time delay in the Kuramoto model of coupled oscillators*, Phys. Rev. Lett. **82**, 648 (1999).
- [22] D. Métivier and S. Gupta, *Bifurcations in the time-delayed Kuramoto model of coupled oscillators: Exact results*, J Stat Phys (2019). <https://doi.org/10.1007/s10955-019-02299-z>
- [23] A. Pollakis, L. Wetzel, D. J. Jörg, W. Rave, G. Fettweis, and F. Jülicher, *Synchronization in networks of mutually delay-coupled phase-locked loops*, New J. of Phys. **16**, 113009 (2014).
- [24] L. Wetzel, D. J. Jörg, A. Pollakis, W. Rave, G. Fettweis, and F. Jülicher, *Self-organized synchronization of digital phase-locked loops with delayed coupling in theory and experiment*, PLOS ONE **12**, e0171590 (2017).
- [25] D. J. Jörg, A. Pollakis, L. Wetzel, M. Dropp, W. Rave, F. Jülicher, and G. Fettweis, *Synchronization of mutually coupled digital PLLs in massive MIMO systems*, IEEE International Conference on Communications (ICC), 15437342 (2015).
- [26] R. Mancini, *Op Amps for Everyone: Design Reference* (Newnes, Oxford, UK, 2003).
- [27] J. K. Hale, *Linear functional differential equations with constant coefficients*, Contributions to Differential Equations **2**, 291 (1963).
- [28] J. K. Hale and S. M. V. Lunel, *Introduction to functional differential equations* (Springer-Verlag, New York, 1993).
- [29] S. Guo and J. Wu, *Bifurcation theory of functional differential equations* (Springer-Verlag, New York, 2013).
- [30] C. Mouhot and C. Villani, *On Landau damping*, Acta Mathematica, **207**, 29 (2011).
- [31] J. D. Crawford, *Amplitude equations for electrostatic waves: Universal singular behavior in the limit of weak instability*, Physics of Plasmas **2**, 97 (1995).
- [32] https://gitlab.pks.mpg.de/lwetzal/all_to_all_pllnetworks, Gitlab (2019).
- [33] H. Hong, H. Chaté, H. Park, and L.-H. Tang, *Entrainment transition in populations of random frequency oscillators*, Phys. Rev. Lett. **99**, 184101 (2007).
- [34] E. Ott and T. M. Antonsen, *Low dimensional behavior of large systems of globally coupled oscillators*, Chaos **18**, 037113 (2008).
- [35] In this work, we use the terms “oscillators” and “rotors” interchangeably.
- [36] Note that in most state-of-the-art electronic systems where synchronization is achieved through entrainment by a reference clock, the phase detector is a *flip-flip* phase-frequency detector, contrary to the XOR component used for the phase detector of the digital PLL’s discussed in this work.